Observed increases in Bering Strait oceanic fluxes from the Pacific to the Arctic from 2001 to 2011 and their impacts on the Arctic Ocean water column

Rebecca A Woodgate[1], Thomas J Weingartner[2], and Ron Lindsay[1]
[1]University of Washington
[2]University of Alaska, Fairbanks
Corresponding Author: Dr R A Woodgate
1013 NE 40th Street, Seattle, WA 98105, USA

Accepted Geophysical Research Letters, November 2012

Key Points:

Bering Strait volume, heat and freshwater fluxes increase ~50% from 2001-2011.
Most of this is due to a ~30% increase in the Pacific-Arctic pressure-head.
Near constant maximum summer salinities set Arctic cold halocline properties.

Abstract

Mooring data indicate the Bering Strait throughflow increases ~50% from 2001 (~0.7Sv) to 2011 (~1.1Sv), driving heat and freshwater flux increases. Increase in the Pacific-Arctic pressure-head explains two-thirds of the change, the rest being attributable to weaker local winds. The 2011 heat flux (~5×10^{20}J) approaches the previous record high (2007) due to transport increases and warmer lower layer (LL) temperatures, despite surface temperature (SST) cooling. In the last decade, warmer LL waters arrive earlier (1.6±1.1 days/yr), though winds and SST are typical for recent decades. Maximum summer salinities, likely set in the Bering Sea, remain remarkably constant (~33.1psu) over the decade, elucidating the stable salinity of the western Arctic cold halocline. Despite this, freshwater flux variability (strongly driven by transport) exceeds variability in other Arctic freshwater sources. Remote data (winds, SST) prove insufficient for quantifying variability, indicating interannual change can still only be assessed by in situ year-round measurements.

Index Terms: 1637,4207,4513,4283, 1621
Keywords: Bering Strait inflow, Pacific-Arctic oceanic fluxes, Arctic cold halocline properties,

1.Introduction

Pacific Waters (PW) dominate about half of the upper Arctic Ocean [*McLaughlin et al.*, 1996]. They provide ~1/3rd of all Arctic freshwater [*Serreze et al.*, 2006]. Supplying 10-20% of the oceanic heat input to the Arctic, warm (summer) PW trigger sea-ice retreat in the western Arctic and provide an under-ice, upper water column heat source [*Woodgate et al.*, 2010]. Cold (winter) PW maintain the western Arctic cold halocline [*Aagaard et al.*, 1981]. In situ measurements from the Bering Strait, the only Pacific-Arctic gateway, showed extreme oceanic fluxes in 2007, which likely influenced that year's precipitous sea-ice retreat [*Woodgate et al.*, 2010]. Given continued Arctic sea-ice retreat and increased Arctic freshwater variability, we consider changes in PW fluxes to 2011.

2. Estimating Bering Strait oceanic fluxes of volume, heat and freshwater

2.1 Data sources

The only oceanic Pacific-Arctic gateway is the ~50m deep, ~85km wide Bering Strait (Figure 1). The flow in the strait is dominantly homogenous, with a surface-intensified, warm, fresh, ~10km wide coastal current (the Alaskan Coastal Current, ACC) present seasonally in the east [*Woodgate et al.*, 2005a and references therein]. Stratification (summer-only) is typically 2-

layer with the upper layer warmer and ~1psu fresher [*Woodgate and Aagaard*, 2005]. Hourly current-meter and temperature-salinity sensor data from year-round moorings in the strait suggest mooring A3, ~60km north of the center of the strait (Figure 1), gives a reasonable average of lower layer flow properties and, with surface and ACC corrections, can be used to infer total fluxes [*Woodgate et al.*, 2006; *Woodgate et al.*, 2010]. We use these techniques to infer Bering Strait oceanic fluxes to 2011 (Figure 1). The strong coherence of velocity in the region allows volume transport also to be estimated from the strait moorings A1 or A2.

Volume transports are calculated from hourly northward velocity (at ~45m depth) at A3 assuming flow homogeneity (laterally and vertically) and a cross-section area of $4.25\times10^6 m^3$. This neglects the ~0.1Sv of the ACC ($1Sv=10^6 m^3/s$) [*Woodgate and Aagaard*, 2005]. A 7-mooring array in the strait deployed from 2007 (not shown) shows that away from the ACC spatial flow variability is <10% and suggests this simplistic transport quantification is reliable to ~0.1Sv, possibly with a systematic bias of <20%.

Heat transports are calculated hourly from a combination of transport and temperature data. Since PW are generally at freezing on leaving the Arctic [*Steele et al.*, 2004], to assess the PW heat contribution to the Arctic we calculate heat fluxes relative to a typical freezing point of Bering Strait waters (-1.9ºC). Lower layer (LL) temperatures are taken from mooring data at ~45m depth. Upper layer temperatures are estimated hourly from the NOAA daily (0.25º spatial resolution) Optimum Interpolation satellite sea surface temperature (SST) product [*Reynolds et al.*, 2007] averaged over a 60kmx80km cross-strait region centered on A3. Heat transports are estimated assuming upper layer thickness of 10m or 20m and a constant annual contribution from the ACC of 1×10^{20}J [*Woodgate et al.*, 2006; *Woodgate et al.*, 2010].

Freshwater transports are also calculated hourly from transport and mooring salinity data from ~45m depth, relative to an Arctic mean salinity of 34.8psu [*Aagaard and Carmack*, 1989]. Lacking long-term sea surface salinity measurements, to account for stratification, the ACC and freshwater from sea-ice transport (~140±40km^3/yr [*Travers*, 2012]) we assume a constant annual contribution of 800-1000km^3/yr [*Woodgate and Aagaard*, 2005; *Woodgate et al.*, 2006] for these terms.

2.2 Annual means from 1991 to 2011

Since 2002 (with one exception, 2005), annual mean (AM) transports (Figure 1) exceed the climatological transport value of 0.8Sv [*Roach et al.*, 1995]. The AM volume transport increases by over 50% from 2001 (~0.7Sv) to 2011 (~1.1Sv). The 2001-2011 trend is 0.03 ± 0.02Sv/yr. (Trend errors in this paper are the 95% level of 1-sided Student's T-test, equivalent to 90% of 2-sided T-test.) There is no significant trend over the 1990-2011 period.

Lower layer AM temperatures are warmer in 2002-2007 and 2010-2011, with 2002, 2003, 2007 and 2011 being the warmest on record. In contrast, AM SSTs are warmest in 2004 and 2007, but for 2008-2011 are cooler, comparable with the 1990s. ACC temperatures (from mooring site A4) are similar to the SST although in 2008 and 2009 ACC temperatures are colder, due at least in part to the current being present for less of the year. Lower layer AM salinities remain within 0.25psu of the climatological value of 32.5psu [*Aagaard and Carmack*, 1989] for all the record, except 1991.

Heat and freshwater (FW) fluxes depend strongly (heat ~50%, FW >90%) on volume flux changes.

The 2007 heat flux, (5-6x10^{20}J/yr, ~15-20TW [*Woodgate et al.*, 2010]) is still the highest recorded, although the 2011 heat flux is also ~5×10^{20}J, despite the surface layer contributing only half as much heat as in 2007. The 2011 heat flux increase is due to increased transport and increased warming of the lower water column not the surface layer.

The freshwater (FW) flux variability here, calculated only from lower layer changes, likely underestimates the real variability, which will reflect ACC and stratification changes. Nevertheless, this estimate suggests Bering Strait FW fluxes increase from 2000-2500km^3 in

2001 to 3000-3500km^3 in 2011. Within a decade, AM values vary by ~1000km^3, roughly twice the variability in net precipitation (~500km^3 [*Serreze et al.*, 2006]) or river run off (Russian rivers,~400km^3 [*Shiklomanov and Lammers*, 2009]) in the same period.

3. What are the drivers of interannual variability?

3.1 Increased transport due to pressure-head and wind changes

The Bering Strait throughflow is attributed to two forcings – a Pacific-Arctic pressure-head term (PH) and the local wind velocity (Wvel) which in the annual mean opposes the northward flow [see e.g., discussion in *Woodgate et al.*, 2005a]. Following *Woodgate et al.,* [2010], we estimate the varying contributions from each by assuming a linear fit – "Transport = PH + C × Wvel", where C is an unknown parameter representing wind-flow coupling. Taking for Wvel the NCEP (National Centers for Environmental Prediction) 10m 6-hourly wind at various strait sites (Figure 1) in the direction best correlated with the water velocity (~330º), we calculate C and PH as coefficients of a least squares fit of Wvel and the estimated transport for 1-year segments of data (Figure 1g,h). Results suggest both forcings increase northward flow from 2001 to 2011 – by increased PH and by (in the annual mean) weaker southward winds. Best fit trends for this period suggest the flow increase due to changes in the PH term (0.024 ± 0.011Sv/yr) is almost twice that due to the weakening of the winds. However, neither term alone indicates all years with maximum flow.

Our results suggest a ~30% increase in the PH term from 2001 to 2011.

3.2 Oceanic warming greater than SST warming

About 50% of the increased heat flux relates to ocean warming: years with large heat fluxes are years with warmer lower layer temperatures (LLTs) (Figure 1c) but not always high SSTs – e.g., 2011 AM SSTs are lower than in 2003-2007 and comparable with the 1990s (Figure 2). An inverse relationship between LLT and SST might reflect increased mixing. Although solar heating warms the upper layer, enhanced vertical mixing will move this heat downward, yielding lower layer warming and upper layer cooling.

Thirty-day smoothed data indicates that recent LLTs rise above 0ºC roughly 20 days earlier than in the late 1990s (1998-2011 trend: 1.6±1.1 days/yr, Figure 2c). This may relate to an observed 3-fold increase in northward transport in recent springs (also seemingly pressure-head driven) speeding advection of heat from the south (not shown). The corresponding trend in SST is not significant (0.8±1.1 day/yr). Although SST rises above 0ºC earlier in the year than LLT (Figure 2c), cooling is coincident throughout the water column (Figure 2d) since the water column is less stratified in autumn [*Woodgate et al.*, 2005b]. There is no significant trend in the onset of cooling. These changes do not contribute greatly to the AM heat flux, which is more strongly influenced by the higher temperatures of the later summer (July-October).

3.3 A multidecadal perspective from remote data?

How remarkable are the recent oceanic flux increases? NCEP wind data since 1948 (Figure 2f,g) suggest that recent winds are uncommon, but not unprecedented. However, wind changes explain only ~1/3rd of the recent transport increase, and there is, so far, no proven way of estimating past variability of the larger PH term prior to the mooring record. While we might expect higher flows in the low wind years of 1989 and the late 1940s, without a better understanding of the processes setting the PH, such extrapolations are dubious.

SST data since 1982 (Figure 2) also show no significant trends, and SST changes are not coincident with LLT changes, showing SST to be of limited use in estimating total heat content. However, the timing of SST autumn cooling does coincide with LLT cooling, suggesting that SSTs may be used as a proxy for the timing of water column cooling.

Thus, currently, in situ measurements remain the only method of estimating Bering Strait oceanic fluxes to the accuracy required to quantify recent interannual change.

4. Impacts on the water column of the Chukchi and the Arctic

The heat flux through the Bering Strait, about 1/3rd of the Fram Strait heat flux, acts as a trigger for sea-ice retreat in the Chukchi and western Arctic and a subsurface source of heat to about half of the Arctic Ocean [*Woodgate et al.*, 2010]. Although upper layers may be significantly modified during transit of the Chukchi, prior data suggest that lower layers are cooled, but undergo remarkably little salinity change [*Woodgate et al.*, 2005a]. We thus consider lower layer water properties at A3 to investigate interannual variability of waters sequestered in the Arctic.

4.1 Two distinct Pacific Water contributions to the Arctic

The temperature-salinity (TS) properties of the lower layer at A3 range from ~29-34psu and from the freezing point (-1.9ºC) to ~8ºC in the period 1998-2011 (Figure 3, first column). Greater insight however comes from considering the volume of water transported through the strait in each TS-class (Figure 3, second column).

In the multiyear mean, two modes are apparent – a Pacific Summer Water (PSW) mode dominantly 1-4ºC, 32-33psu, and a Pacific Winter Water (PWW) mode at the freezing temperature but with a greater salinity range ~31.5-33.5psu. (This analysis neglects the warmer, fresher upper layers which are 10%-20% of the volume – 10-20m layer present half the year.) These modes are of roughly equal volume, consistent with the seasonal cycle of temperature (warm ~ June to December) being offset from the seasonal cycle of transport (high transports ~ April to September) [*Woodgate et al.*, 2005b]. It is perhaps surprising that the salinities of these modes overlap (Figure 3, third column) – especially in recent warm years (2007 and 2011), warm waters are found at salinities greater than much of the PWW. There is significant interannual variability in the temperatures and TS distributions of the PSW. High salinities in PWW are rarer in recent times.

Remarkably, for all the period 1998 to 2011, waters above 0ºC exhibit a sharp cutoff in salinity, being always fresher than 33.1psu. Summer waters may be fresher than this salinity, but higher salinities are only found in cold (<0ºC) waters. Even then the salinity change is modest (<1psu), consistent with formation of <2m of ice in 50m of water. (Mean Bering Strait ice thickness for 2007 is ~1.5m [*Travers*, 2012].) The 33.1psu salinity cutoff suggests a quasi-constant maximum salinity source for PSW, likely relating to shelf break depth upstream in the Bering Sea – indeed monthly National Ocean Data Center climatological salinities show that at 50m most of the Bering Sea Basin is ~33-33.2psu, with fresher waters on the shelf.

4.2 A Pacific control on temperatures and salinities of the Arctic halocline?

The western Arctic Ocean water column TS is characterized by a contraction in temperature towards freezing at a salinity (~33.1psu) which is remarkably constant over recent decades [e.g., Figure 2 of *Woodgate et al.*, 2005c]. The sharp salinity cutoff for Bering Strait warm waters may explain this – there is no source of waters with significant heat at salinities ~ 33.1 psu since Atlantic waters are too salty and, as found here, Pacific waters at these salinities (or higher) are always cold. Thus suggests the constancy of this Arctic property is set by conditions in the Bering Sea.

Note that in the western Arctic, the term Pacific Summer Water (henceforth APSW) refers to the temperature maximum (Tmax) in salinity range 31-33psu above this TS contraction [*Steele et al.*, 2004], e.g., Figure 3 (temperature maximum in yellow lines). However, a comparison with TS from the Chukchi (Figure 3) indicates that the APSW Tmax is actually only a cooled remnant of the deeper part of the warm Bering Strait/Chukchi Sea PSW. Thus spatial and temporal variability of the APSW Tmax depends not just on source changes and likely changing pathways but also on the processes removing heat from the upper part of the Pacific Waters.

4.3 Pacific water contribution to heat in the Arctic water column

Finally, we consider where Bering Strait heat may be stored in the Arctic. Figure 3 (fourth column) shows the heat flux per density class entering through the strait. The upper layers (missing from this summation) contribute heat at lower densities. The summation presented indicates that between 0.2 to 0.6×10^{20}J/yr are contributed at sigma-0 values around 26kg/m^3, equating to a ventilation depth of 50-75m in the Arctic Ocean.

5 Conclusions

Mooring data indicate a >50% increase in the Bering Strait throughflow from 2001 (~0.7Sv) to the end of the present record in 2011 (~1.1Sv), and combined with NCEP wind data, suggest that 2/3rds of this increase is attributable to an increase in the Pacific-Arctic pressure-head. Predicting future changes in the Bering Strait throughflow thus requires understanding of the origin and variability of this pressure-head.

Making a 2-layer assumption and assuming a constant Alaskan Coastal Current (ACC) contribution, we estimate heat and freshwater fluxes, both of which depend strongly (heat ~50%; freshwater>90%) on transport changes. Freshwater fluxes rise from 2000-2500km^3 in 2001 to 3000-3500km^3 in 2011, and exhibit interannual variations of ~1000km^3, which is larger than the interannual variability in other Arctic freshwater sources. Our assumptions likely underestimate the true variability, since stratification and the ACC contribute about 1/3rd of the flux. Heat fluxes increase from ~3x10^{20}J in 2001 to ~5x10^{20}J in 2011 (comparable to the record of 2007). Again this also probably understimates variability – ACC temperatures (A4 in Figure 1c) show more variability than Sea Surface Temperatures (SSTs). Lower layer temperatures (although not SSTs) suggest that Bering Strait waters warmed earlier from 2001 to 2011 (1.6±1.1 days/yr), possibly relating to increased transport of warm water from the south in the spring. The onset of autumn cooling, coherent over the water column, shows no significant change over time.

The 2011 Bering Strait heat flux is enough to melt ~1.5x10^{6}km^2 of 1m thick ice. A volumetric analysis of water properties shows that significant quantities of heat (0.2 to 0.6×10^{20}J/yr) are associated with surprisingly high densities (σ_0 ~26kg/m^3), suggesting an Arctic ventilation depth of 50-75m. About equal volumes of cold (<0ºC) and warm (>0ºC) waters are supplied to the Arctic. Interestingly, despite large variations in temperature (~2ºC), Pacific Summer Water salinities never exceed 33.1psu in the record available. This curiously stable maximum salinity, likely with origins in the Bering Sea, may explain the stable salinity of the western Arctic cold halocline.

Local winds and SST miss much of the variability important for quantifying the Bering Strait oceanic fluxes, viz., the pressure-head forcing and temperature variability at depth. Thus, in situ observations remain currently the only viable method of assessing interannual change in the Pacific inflow to the Arctic.

Acknowledgments

This work was funded by NSF (ARC-0632154 and ARC-053026) with ship-time from NOAA-RUSALCA. We thank J.Johnson, D.Leech and the scientists and crews of the Alpha Helix, the CCGC Sir Wilfrid Laurier, and the Russian vessels Khromov, Sever, and Lavrentiev for their dedication to fieldwork; M.Schmidt for MODIS imagery; NOAA/OAR/ESRL PSD Boulder Colorado for the NOAA-High Resolution SST data (http://www.esrl.noaa.gov/psd); and NODC for Bering Sea climatology data (http://www.nodc.noaa.gov/OC5/PACIFIC2009/index.html) .

Figures:

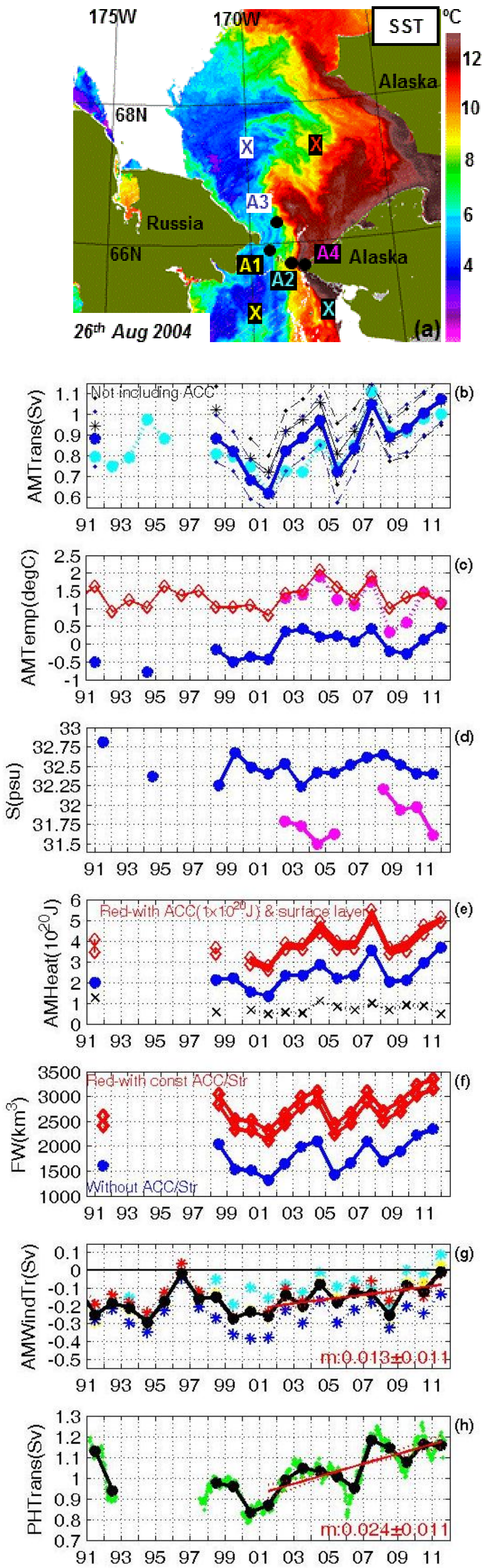

Figure 1 (a) A Bering Strait summer satellite (MODIS) Sea Surface Temperature (SST) image marking moorings (black dots) and NCEP wind points (X) [from *Woodgate et al.*, 2010].

(b-h) Bering Strait annual mean (AM) time-series from 1991 – 2011 of:

b) transport calculated from A3 (blue) or A2 (cyan), with error bars (dashed) calculated from variability; including adjustments estimated from 2007-2009 Acoustic Doppler Current Profiler data for 6-12m changes in instrument depth (black);

c) near-bottom temperatures from A3 (blue) and A4 (magenta-dashed), and the NOAA SST product (red diamonds);

d) salinities from A3 (blue) and A4 (magenta);

e) heat fluxes: blue - from A3 only; red – including ACC correction (1×10^{20}J) and contributions from surface layer of 10m (lower bound) or 20m (upper bound) at SST, with black x indicate heat added from 20m surface layer;

f) freshwater fluxes: blue – from A3 only; red – including 800-1000km^3 (lower and upper bounds) correction for stratification and ACC;

g) transport attributable to NCEP wind (heading 330º, i.e., northwestward) at each of 4 points (coloured X in **(a)**) and the average thereof (black); and

h) transport attributable to the pressure-head term from the annual (black) or weekly (green) fits.

Uncertainties are order 10-20%. Red lines on **(g)** and **(h)** indicate best fit for 2001-2011 (trends=m±error, in Sv/yr, error being the 95% confidence limit from a 1-sided Student's t-test).

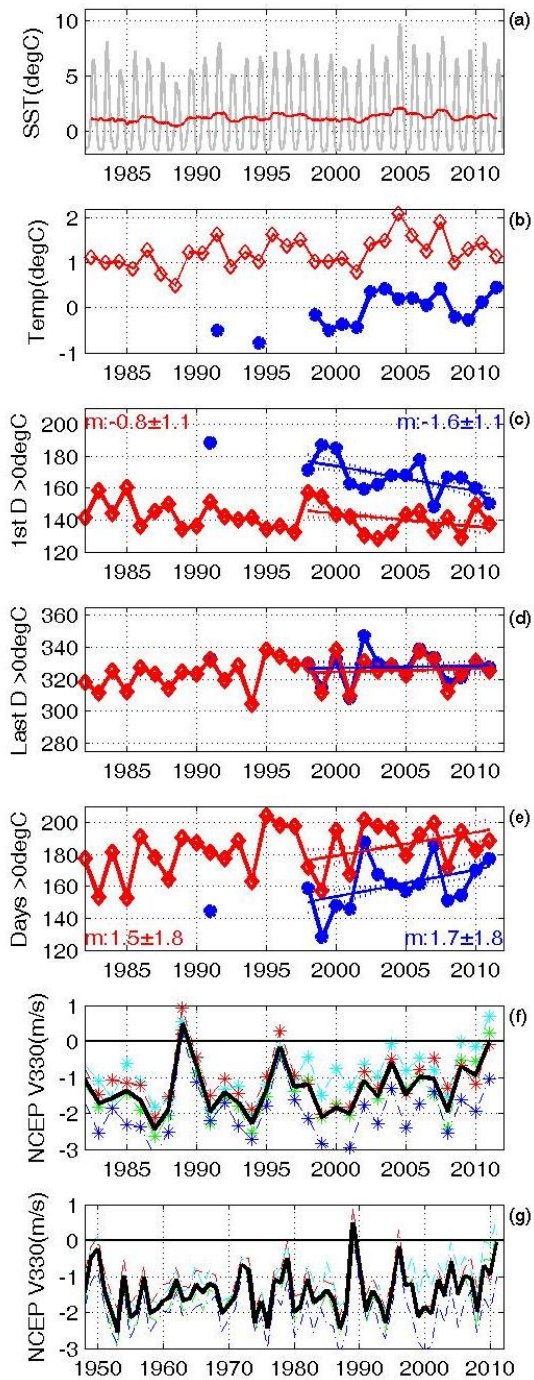

Figure 2: Time-series of:
a) 30-day (grey) and 365-day (red) smoothed NOAA SST data for the Bering Strait region;
b) annual mean SST (red diamonds) and A3 lower layer (LL) temperature (blue dots);
c) first day in year when 30-day smoothed SST (red diamonds) or A3 LL temperature is above 0ºC, with trends (as per Figure 1) in days/yr for 1998-2011 for SST (top left) and A3 (top right);
d) as per (c) for last day in year when temperatures above 0ºC (trends are not significant);
e) as per (c) for number of days above 0ºC;
f) and **(g)** annual mean NCEP winds at heading 330º (i.e., northwestward) at each of 4 points (coloured X in Figure 1a) and the average thereof (black) for 1982-2011 **(f)** and 1948-2011 **(g)**.

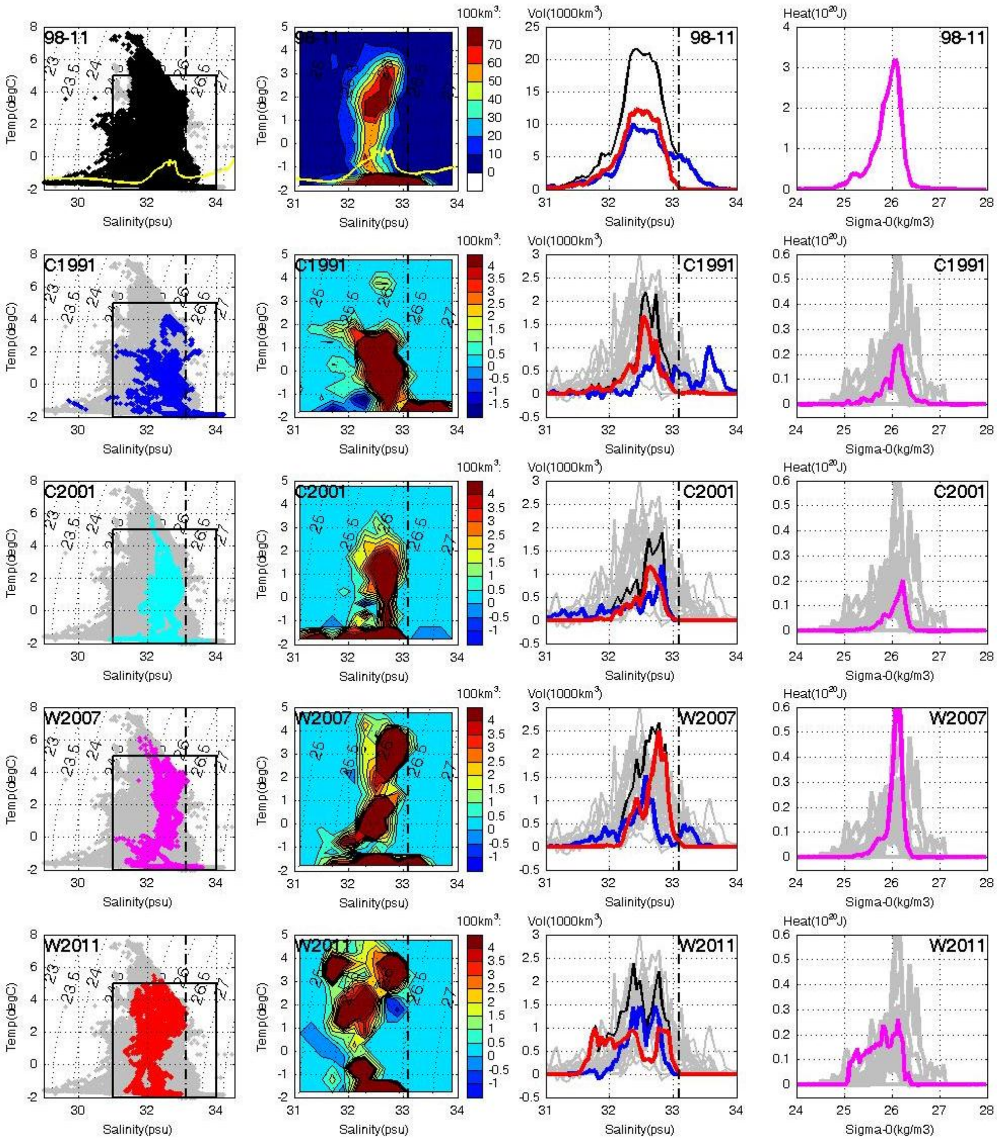

Figure 3: Bering Strait temperature-salinity (TS) and volume information inferred from A3. (ACC and straitification (neglected) add ~ 10-20% of the total volume to lower densities.)

First row: Hourly A3 lower layer (LL, ~45m depth) data from 1998 to 2011. **Rows 2-5:** A3 LL data from cold years 1991 **(row 2)** and 2001 **(row 3)** and warm years 2007 **(row 4)** and 2011 **(row 5)**.

First column: Temperature-salinity (TS) plot with sigma-0 contours showing that year's data (in color) and 1998-2011 data (grey). Black box marks extract of TS plot shown in column 2. Yellow line is a western Arctic TS profile from 2002 (CBL2002 station 14 - 76º31.4'N, 168º51.8W in 750m water north of the Chukchi slope [*Woodgate et al.*, 2005c]).

Second column: Volume of water (in TS classes) for that year (or group of years) infered from moored velocity measurements. Positive/Negative values indicate net northward/southward transport.

Third column: Volume of water per salinity class for that year (or group of years) above 0ºC (red), below 0ºC (blue), and total (black). Grey lines indicate totals from each year 1998-2011.

Fourth column: Heat flux per sigma-0 class for that year (or group of years). Grey lines indicate totals from each year 1998-2011.

In first 3 columns, black dashed line marks 33.1 psu.

References:

Aagaard, K., and E. C. Carmack (1989), The role of sea ice and other fresh water in the Arctic circulation, *J. Geophys. Res.*, *94*(C10), 14485-14498.

Aagaard, K., L. K. Coachman, and E. Carmack (1981), On the halocline of the Arctic Ocean, *Deep-Sea Res., Part A*, *28*(6A), 529-545.

McLaughlin, F. A., E. C. Carmack, R. W. Macdonald, and J. K. B. Bishop (1996), Physical and geochemical properties across the Atlantic/Pacific water mass front in the southern Canadian basin, *J. Geophys. Res.*, *101*(C1), 1183-1197.

Reynolds, R. W., T. M. Smith, C. Liu, D. B. Chelton, K. S. Casey, and M. G. Schlax (2007), Daily high-resolution-blended analyses for sea surface temperature, *J. Climate*, *20*(22), 5473-5496, doi: 10.1175/2007jcli1824.1.

Roach, A. T., K. Aagaard, C. H. Pease, S. A. Salo, T. Weingartner, V. Pavlov, and M. Kulakov (1995), Direct measurements of transport and water properties through the Bering Strait, *J. Geophys. Res.*, *100*(C9), 18443-18457.

Serreze, M. C., A. P. Barrett, A. G. Slater, R. A. Woodgate, K. Aagaard, R. B. Lammers, M. Steele, R. Moritz, M. Meredith, and C. M. Lee (2006), The large-scale freshwater cycle of the Arctic, *J. Geophys. Res.*, *111*, C11010, doi: 10.1029/2005JC003424.

Shiklomanov, A. I., and R. B. Lammers (2009), Record Russian river discharge in 2007 and the limits of analysis, *Environmental Research Letters*, *4*(4), 045015, doi: 10.1088/1748-9326/4/4/045015.

Steele, M., J. Morison, W. Ermold, I. Rigor, M. Ortmeyer, and K. Shimada (2004), Circulation of summer Pacific halocline water in the Arctic Ocean, *J. Geophys. Res.*, *109*(C2), C02027, doi: 10.1029/2003JC002009.

Travers, C. S. (2012), Quantifying Sea-Ice Volume Flux using Moored Instrumentation in the Bering Strait, 85 pp, University of Washington.

Woodgate, R. A., and K. Aagaard (2005), Revising the Bering Strait freshwater flux into the Arctic Ocean, *Geophys. Res. Lett.*, *32*(2), L02602, doi: 10.1029/2004GL021747.

Woodgate, R. A., K. Aagaard, and T. J. Weingartner (2005a), A year in the physical oceanography of the Chukchi Sea: Moored measurements from autumn 1990-1991, *Deep-Sea Res., Part II*, *52*(24-26), 3116-3149, doi: 10.1016/j.dsr2.2005.10.016.

Woodgate, R. A., K. Aagaard, and T. J. Weingartner (2005b), Monthly temperature, salinity, and transport variability of the Bering Strait throughflow, *Geophys. Res. Lett.*, *32*(4), L04601, doi: 10.1029/2004GL021880.

Woodgate, R. A., K. Aagaard, and T. J. Weingartner (2006), Interannual Changes in the Bering Strait Fluxes of Volume, Heat and Freshwater between 1991 and 2004, *Geophys. Res. Lett.*, *33*, L15609, doi: 10.1029/2006GL026931.

Woodgate, R. A., T. J. Weingartner, and R. W. Lindsay (2010), The 2007 Bering Strait Oceanic Heat Flux and anomalous Arctic Sea-ice Retreat, *Geophys. Res. Lett.*, *37*, L01602, doi: 10.1029/2009GL041621.

Woodgate, R. A., K. Aagaard, J. H. Swift, K. K. Falkner, and W. M. Smethie (2005c), Pacific ventilation of the Arctic Ocean's lower halocline by upwelling and diapycnal mixing over the continental margin, *Geophys. Res. Lett.*, *32*(18), L18609, doi: 10.1029/2005GL023999.